Chin. J. Chem. Eng., **15**(5) 765—771 (2007)
RESEARCH NOTES

Correlation of Vapour Liquid Equilibria of Binary Mixtures Using Artificial Neural Networks

Hajir Karimi[a,*] **and Fakhri Yousefi**[b]
[a] Chemical Engineering Department, Yasouj University, Yasouj 75914-353, Iran
[b] Department of Chemistry, College of Science, Shiraz University, Shiraz 71454, Iran

Abstract In this paper, a back propagation artificial neural network (BP-ANN) model is presented for the simultaneous estimation of vapour liquid equilibria (VLE) of four binary systems *viz* chlorodifluoromethan-carbondioxide, trifluoromethan-carbondioxide, carbondisulfied-trifluoromethan and carbondisulfied-chlorodifluoromethan. VLE data of the systems were taken from the literature for wide ranges of temperature (222.04—343.23K) and pressure (0.105 to 7.46MPa). BP-ANN trained by the Levenberg-Marquardt algorithm in the MATLAB neural network toolbox was used for building and optimizing the model. It is shown that the established model could estimate the VLE with satisfactory precision and accuracy for the four systems with the root mean square error in the range of 0.054—0.119. Predictions using BP-ANN were compared with the conventional Redlich-Kwang-Soave (RKS) equation of state, suggesting that BP-ANN has better ability in estimation as compared with the RKS equation (the root mean square error in the range of 0.115—0.1546).
Keywords vapour liquid equilibria, artificial neural networks, refrigerant

1 INTRODUCTION

In the process modeling, design and simulation, it is important to have accurate data on physical properties such as vapour liquid equilibria (VLE) of the compounds involved in the studied system. Several conventional thermodynamic models such as equations of state (EoS) are used for estimating the VLE. The modeling with acceptable VLE prediction by EoS requires the use of many adjustable parameters or mixing rules. Therefore, using EoS for estimating the VLE is boring and requires an iterative method that may sometimes poses problem for real time control of an operating plant. In such cases, other faster alternative methods would be more interesting. In recent years, artificial neural network (ANN) has shown to be very successful in modeling complex non-linear systems and providing precise data extraction from measurement.

Nowadays, ANN has found extensive application in the field of thermodynamics and transport properties such as estimation of VLE[1—7], viscosity[8,9], density[10], vapour pressure[11], compressibility factor[10] and thermal conductivity[12] *etc*. This method provides non-linear function mapping of a set of input variables into the corresponding network output, without the requirement of specifying the actual mathematical form of the relation between the input and output variables. Due to its flexibility and parallel structure even in the presence of significant amounts of noise in the input data, ANNs can be applied for accurate determination VLE of polar and nonpolar components. Basic theory and application to chemical problems of ANN with the back-propagation algorithm is well discussed in [13—18].

A back propagation artificial neural network model is presented in this article for accurate prediction of VLE for four binary refrigerant systems: chlorodifluoromethan - carbondioxide (R22-CO_2), trifluoromethan-carbondioxide (R23-CO_2), carbondisulfied-chlorodifluoromethan (CS_2-R22) and carbondisulfied-trifluoromethan (CS_2-R23). The performance characteristics of the proposed ANN models were compared with the conventional EoS (*i.e*. Redlich-Kwong-Soave equation as a typical representative of empirical equations of state). Experimental data needed for development of the ANN model were taken from Ref.[19].

2 ARTIFICIAL NEURAL NETWORK THEORY

Neural networks consist of arrays of simple active units linked by weighted connections (Fig.1). ANN consists of multiple layers of neurons arranged in such a way that each neuron in one layer is connected with each neuron in the next layer. The network used in this paper is a multilayer feed forward neural network with a learning scheme of the back-propagation (BP) of errors and the Levenberg-Marquardt algorithm[14] for the adjustment of the connecting weights. Neurons are the fundamental processing element of an ANN[20], which are arranged in layers that make up the global architecture.

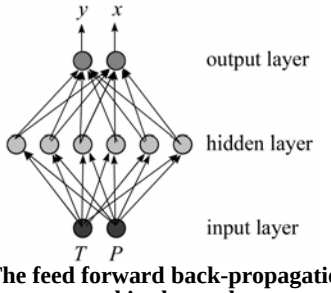

Figure 1 The feed forward back-propagation network used in the study
[*T* and *P* of a system are chosen as input data, *x* and *y* (mole fraction of a component in liquid and vapour phases) as output data]

Received 2007-03-06, accepted 2007-06-28.
* To whom correspondence should be addressed. E-mail: hakar@mail.yu.ac.ir

BP networks are usually comprised of one input layer, at least one hidden layer and an output layer. The number of neurons in the input and output layers is defined by the problem to be solved. The input layer receives the experimental information, experimental parameters, structural descriptions *etc*. The output layer delivers the response sought for the property value, classification *etc*. The hidden layer encodes and organizes the information received from the input layer and delivers it to the output layer.

The number of neurons in the hidden layer, which to some extent play the role of intermediate variables, may be considered as an adjustable parameter. Each neuron thus has a series of weighted inputs, w_{ij} which might be either output from other neurons or input from external sources. Each neuron calculates a sum of the weighted inputs and transforms it by a Sigmoid transfer function:

$$a_j = \frac{1}{1+\exp(-n)} \tag{1}$$

where a_j the output from the jth neuron is connected to ith neuron in the previous layer, and n is in turn given by

$$n = \sum_{i=1}^{n} w_{ij} p_i + b_j \tag{2}$$

where w_{ij} represents the weights applied to the connections from ith to jth neurons. p_i is the output from the ith neuron in the previous layer and b_j is a bias term. BP networks operate in the supervised learning mode. In the first step (training), known data are given to the networks and using the BP algorithm, the network iteratively adjusts the connection weights w_{ij} and biases b_j (starting from initial random values) until the predicted output satisfactorily match the actual data. In the BP training algorithm this adjustment is carried out by comparing the experimental data t_{ij} and the current output a_{ij} of the network in terms of the total sum of the square error (*SSE*) for the k patterns of the learning set:

$$SSE = \sum_{i=1}^{k} \left(t_{ij} - a_{ij}\right)^2 \tag{3}$$

The weights adjusted in the training stage for all the interconnections can then be used for the prediction of output values from any input in the test set.

3 METHODOLOGY

3.1 Experimental data

The first step in modelling is compiling the database to train the network and to evaluate its ability for generalization. Many researchers measured VLE data by various techniques. Comprehensive review on the VLE data has also been published[21]. In the present work, experimental VLE data in the temperature range of 222.04—343.23K and the pressure range from 0.105 to 7.46MPa for four binary systems were taken from Roth *et al*.[19] and were used for training and validating the ANN model. The temperature, pressure and mole fraction of the vapour liquid phases reported by these authors are summarized in Table 1.

Table 1 Data and range used for development of the ANN model

System	Temperature, K	Pressure, MPa	Mole fraction CO_2 in vapour	Mole fraction CO_2 in liquid	No. of data points[19]
R22-CO_2	273.15	0.789—3.176	0.1236—09175	0.4072—0.976	52
	298.15	1.571—5.749	0.1361—0.9153	0.3656—0.9587	
	313.15	1.978—6.556	0.0919—0.7876	0.2387—0.8649	
	328.15	2.762—7.015	0.0964—0.6538	0.216—0.728	
	348.15	4.135—6.550	0.1071—0.3876	0.1853—0.4388	
	358.15	4.190—5.740	0.0205—0.2008	0.0344—0.2465	
R23-CO_2	254.15	1.499—1.990	0.0753—0.9227	0.1025—0.9328	41
	263.15	1.953—2.628	0.0469—0.9279	0.0621—0.9377	
	273.15	2.594—3.425	0.0526—0.8458	0.0668—0.8655	
System	Temperature, K	Pressure, MPa	Mole fraction R23 in vapour	Mole fraction R23 in liquid	No. of data points[19]
CS_2-R23	273.2	0.355—2.409	0.006—0.963	0.9443—0.988	103
	298.2	0.410—4.514	0.006—0.97	0.8756—0.9814	
	303.2	0.507—20.540	0.009—0.06	0.8743—0.9681	
	323.2	0.820—19.780	0.010—0.0868	0.8458—0.9496	
	348.2	1.010—29.740	0.011—0.143	0.7401—0.9149	
	373.2	0.970—22.590	0.007—0.207	0.5056—0.8701	
	398.2	1.520—22.370	0.009—0.404	0.4510—0.8215	
	423.2	2.040—18.060	0.01—0.386	0.3320—0.7314	

Table 1 (Continued)

System	Temperature, K	Pressure, MPa	Mole fraction R23 in vapour	Mole fraction R23 in liquid	No. of data points[19]
CS_2-R23	448.2	2.270—16.310	0.006—0.359	0.1403—0.6400	103
	473.2	3.550—14.660	0.011—0.304	0.1779—0.5128	
System	Temperature, K	Pressure, MPa	Mole fraction R22 in vapour	Mole fraction R22 in liquid	No. of data points[19]
CS_2-R22	273	0.106—0.451	0.0332—0.8886	0.6309—0.9724	85
	298	0.226—0.895	0.0358—0.7834	0.7811—0.9579	
	323	0.462—1.843	0.0505—0.9386	0.7445—0.9782	
	348	0.394—3.139	0.0165—0.9438	0.3884—0.9740	
	373	0.601—4.965	0.0137—0.9389	0.2565—0.9550	
	398	1.499—5.890	0.0476—0.7492	0.4656—0.8084	
	423	1.680—6.745	0.0249—0.5764	0.2485—0.7012	
	448	2.070—7.600	0.0116—0.4668	0.0919—0.5921	

3.2 ANN modeling

A multi-layer feed forward network structure was used in this study as shown in Fig.1. ANN modeling was carried out by employing the custom neural network toolbox developed in MATLAB ver.7. The input layer has two neurons for T and P of the system and two neurons are in the output layer corresponding to the vapour and liquid composition of interested components in the binary mixture. The input and output layer nodes had a linear transfer function (purline) while only the hidden layer nodes had sigmoid transfer function for the ANN model. The raw input data need to be preprocessed to convert them to a suitable form. Thus, all input and target data were scaled to a similar magnitude in the range [−1, 1] by the function "premnmx" was developed in MATLAB toolbox. ANNs were trained according to the Levenberg-Marquardt algorithm available in the neural network toolbox of MATLAB.

3.3 RKS correlation

The Redlich-Kwong-Soave equation was considered as a typical representative of empirical equations of state. In order to apply this equation of state to mixtures the Redlich-Kwong-Soave (RKS) equation in Ref.[22] was used. The adjustable parameters of equation (*i.e.* pure-fluid and binary interaction parameters) were taken from Roth *et al*.[19].

3.4 Evaluation of models

All trained ANNs with different configurations and the RKS correlation were evaluated for there modeling capability by validating data. Root mean square error (*RMSE*) and mean absolute error defined by Eqs.(4) and (5) respectively were evaluated for vapor liquid composition of CO_2 corresponding to R22-CO_2 and R23-CO_2 mixtures and R22 corresponds to CS_2-R22 and CS_2-R23 systems. The correlation coefficient, R^2, of the linear regression between the predicted values from the ANN models and the experimental data evaluated by Eq.(6) was also used as a measure of the prediction performance.

$$MAE = \frac{1}{m}\sum_{i=1}^{n}\frac{\left|v_i^{\text{act}} - v_i^{\text{cal}}\right|}{v_i^{\text{act}}} \tag{4}$$

$$RMSE = \left[\frac{\sum_{s=1}^{r}\sum_{i=1}^{m}\left(\frac{v_i^{\text{act}} - v_i^{\text{cal}}}{v_i^{\text{act}}}\right)^2}{rm}\right]^{1/2} \tag{5}$$

$$R^2 = \frac{l_{\text{pt}}}{\sqrt{l_{\text{pp}} l_{\text{u}}}} \tag{6}$$

with

$$l_{\text{pp}} = \sum_{i=1}^{n}\left(v_i^{\text{cal}} - \overline{v}^{\text{cal}}\right)^2 \qquad l_{\text{tt}} = \sum_{i=1}^{n}\left(v_i^{\text{act}} - \overline{v}^{\text{act}}\right)^2$$

$$l_{\text{pt}} = \sum_{i=1}^{n}\left(v_i^{\text{cal}} - \overline{v}^{\text{cal}}\right)\left(v_i^{\text{act}} - \overline{v}^{\text{act}}\right)$$

In Eq.(4), m is the number of test data, v^{act} is the experimental value, v^{cal} is the calculated value using ANN. In Eq.(5) r is the overall input variables of the test data and m is the overall output variables.

4 RESULTS AND DISCUSSION

4.1 ANN models

Using the random selection method, 80% of all data were assigned to the training set, while the rest of data were used as the validation set. In training phase, the number of neurons in hidden layer was important to the network optimization. However, decision on the number of hidden layer neurons is difficult because it depends on the specific problem being solved using ANN. With too few neurons, the network may not be powerful enough for a given learning task. With a

large number of neurons, the ANN may memorize the input training data very well so that the network tends to perform poorly on new test data and is called "over-fitting". Therefore, the optimization of ANN started with 2 neurons in the hidden layer and gradually increasing the number till no significant improvement in performance of the network was further achieved. The performance criterion was the mean square error (*MSE*) when the test data set fed to the trained network. The characteristics of the optimized networks used to modeling for various binary systems are summarized in the Table 2. For the R22-CO_2, CS_2-R22, R23-CO_2 and CS_2-R23 systems, the numbers of neurons in the hidden layer were 5, 6, 8, and

Table 2 The characteristics of the optimized networks used to modeling for various binary systems

System	ANN Parameters			R^2	
	No. of neurons in hidden layer	Transfer function		Vapor	Liquid
		Hidden layer	Output layer		
R22-CO_2	5	sigmoid	purline①	0.999	0.998
R23-CO_2	6	sigmoid	purline	0.997	0.996
CS_2-R22	8	sigmoid	purline	0.997	0.996
CS_2-R23	10	sigmoid	purline	0.998	0.990

① A linear transfer functions calculate a layer's output from its net input n [purline(n)=n].

Table 3 ANN weight connectivity for the hidden and output layers of four systems

Hidden layer connectivity

R22-CO_2			CS_2-R22			R23-CO_2			CS_2-R23		
w_{ji}		b_j	w_{ji}		b_j	w_{ji}		b_j	w_{ji}		b_j
0.27719	−0.76258	−2.2875	−0.29002	0.49384	1.7008	0.087545	0.63494	−0.66586	−0.40733	0.34064	0.54584
−0.10944	−0.11325	0.17392	−2.0203	0.72564	−2.651	9.206	−10.295	1.3515	0.62724	−0.0987	0.007808
−10.728	3.9217	−7.3499	1.9647	−0.35245	2.856	0.84901	−0.52627	0.070318	−0.48499	0.59563	0.21494
0.37947	−0.11756	−0.29769	0.27356	0.21652	−0.51822	0.031072	0.27454	0.09015	−2.8109	3.8605	−3.7779
−0.11157	0.23064	−0.12803	−1.6811	1.8474	−1.0426	−6.5249	−2.6639	−4.9048	0.4972	1.0513	−2.9433
			1.6831	−1.9077	1.1235	1.4314	3.4049	0.31072	−43.482	10.42	−37.08
						0.20623	−1.5536	−2.4445	−39.323	9.523	−34.206
						−35.088	32.452	−15.214	0.61004	−3.4796	−4.7914
									42.561	−11.044	38.24
									0.19124	1.4534	-3.8228

Output layer connectivity

R22-CO_2

w_{ji}					b_j
−5.7885	28.391	−0.13273	12.187	23.251	−4.1755
−10.678	−5.2105	0.017877	−6.5214	−3.9751	−11.634

CS_2-R22

w_{ji}						b_j
3.114	52.069	45.212	−0.04138	15.461	14.595	3.9251
24.432	4.5932	4.1904	−3.619	−5.0208	−5.0291	−23.497

R23-CO_2

w_{ji}								b_j
−8.2446	−0.16674	−4.2298	22.966	0.6366	−0.41232	1.3719	5.8997	2.0173
−2.5281	−0.1161	−4.8269	8.8695	0.062802	0.084998	−3.9454	5.0405	−0.14661

CS_2-R23

w_{ji}										b_j
0.75864	0.81053	0.45521	−0.20205	6.2024	−14.511	45.138	−0.2325	30.629	−4.3643	0.72852
7.4642	0.45646	−3.6492	0.090791	−6.8833	−0.26738	0.84208	−3.6354	0.5619	4.6376	−8.1605

10 neurons respectively. All the weights for models are shown in Table 3. The predicted VL mole fractions of interested component in the all-binary mixtures *versus* their actual VL mole fractions were showed in Figs.2—5. All figures show the modelling ability of the optimized ANN. The R^2 values listed in Table 2 suggest that the accuracy of the ANN prediction is quite satisfactory.

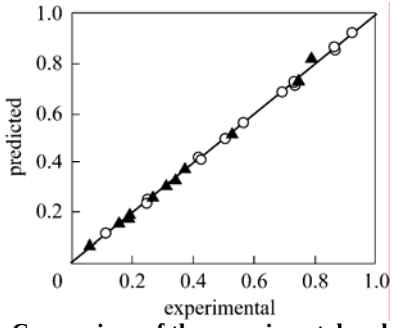

Figure 2 Comparison of the experimental and predicted mole fraction of CO_2 for R22-CO_2 system for the test data
mole fraction of CO_2: ○ in vapor, R^2=0.999, *MAE*=0.62%; ▲ in liquid, R^2=0.998, *MAE*=1.36%

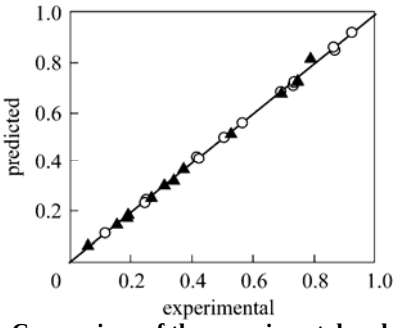

Figure 3 Comparison of the experimental and predicted mole fraction of R22 for CS_2-R22 system for the test data
mole fraction of R22: ○ in vapor, R^2=0.997, *MAE*=1.78%; ▲ in liquid, R^2=0.996, *MAE*=3.26%

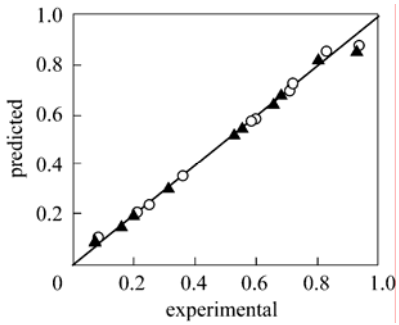

Figure 4 Comparison of the experimental and predicted mole fraction of CO_2 for R23-CO_2 system for the test data
mole fraction of CO_2: ○ in vapor, R^2=0.997, *MAE*=2.21%; ▲ in liquid, R^2=0.996, *MAE*=1.93%

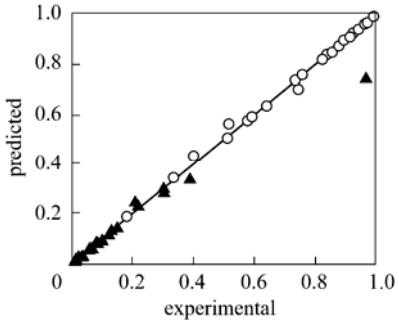

Figure 5 Comparison of the experimental and predicted mole fraction of R23 for CS_2-R23 system for the test data
mole fraction of R23: ○ in vapor, R^2=0.998, *MAE*=1.53%; ▲ in liquid, R^2=0.990, *MAE*=5.15%

4.2 Comparison with RKS correlation

Comparison of ANN and RKS analyses is given in Table 4, where the vapour and liquid mole fractions for all binary systems calculated by means of the respective models and experimental values are tabulated. These results show the predictive ability of models when applied to the validation set. It is immediately

Table 4 Results obtained for validation set modeled with ANN and RKS correlation for four binary system, at wide rang of temperature and pressure with respective errors

System	Temperature, K	Pressure, MPa	Mole fraction CO_2 in vapour			Mole fraction CO_2 in liquid			*RMSE*	
			Exp.	ANN predicted	RKS predicted	Exp.	ANN predicted	RKS predicted	ANN	RKS
R22-CO_2	273	1.440	0.7340	0.7221	0.7440	0.3730	0.3820	0.3760	0.059	0.115
		2.550	0.9217	0.9284	0.9250	0.7435	0.7395	0.7480		
	328	4.190	0.5027	0.5004	0.5060	0.3069	0.3132	0.3200		
		6.210	0.6894	0.6850	0.6950	0.5610	0.5655	0.5730		
	358	4.650	0.1155	0.1152	0.1130	0.0605	0.0728	0.0829		
		5.640	0.2433	0.2393	0.2340	0.1865	0.1867	0.2120		
R23-CO_2	273	2.898	0.3088	0.3076	0.3390	0.3610	0.3597	0.3890	0.150	0.436
		3.295	0.6815	0.6896	0.6310	0.7208	0.7337	0.7110		
		2.594	0.0526	0.0538	0.0638	0.0668	0.0693	0.1480		
		4.345	0.0709	0.0930	0.0638	0.0822	0.1116	0.1310		
	293	5.190	0.5523	0.5538	0.5340	0.5877	0.5824	0.5740		

Table 4 (Continued)

System	Temperature, K	Pressure, MPa	Mole fraction R23 in vapour			Mole fraction R23 in liquid			*RMSE*	
			Exp.	ANN predicted	RKS predicted	Exp.	ANN predicted	RKS predicted	ANN	RKS
CS_2-R23	273	0.994	0.9777	0.9753	0.9800	0.0172	0.0174	0.0242	0.039	0.151
		2.194	0.9844	0.9873	0.9960	0.0342	0.0318	0.0403		
		2.409	0.9880	0.9866	0.9830	0.9628	0.0340	0.9720		
	348	7.020	0.9149	0.9089	0.8960	0.0829	0.0812	0.0803		
		19.960	0.8358	0.8379	0.7270	0.1315	0.1307	0.1120		
	473	10.010	0.5128	0.5055	0.4740	0.1202	0.1162	0.1160		
		14.660	0.3957	0.4327	0.4260	0.3043	0.2831	0.2370		

System	Temperature, K	Pressure, MPa	Mole fraction R22 in vapour			Mole fraction R22 in liquid			*RMSE*	
			Exp.	ANN predicted	RKS predicted	Exp.	ANN predicted	RKS predicted	ANN	RKS
CS_2-R22	348	0.942	0.7341	0.7343	0.7190	0.0773	0.0985	0.0812		
		3.139	0.9740	0.9633	0.9790	0.9438	0.9606	0.9550		
		2.016	0.8713	0.8759	0.8740	0.3643	0.3751	0.3840		
	398	4.075	0.7650	0.7683	0.7680	0.3540	0.3547	0.3550	0.119	0.546
		1.499	0.4656	0.4789	0.4310	0.0476	0.0556	0.0446		
	473	5.300	0.3906	0.4074	0.1080	0.1257	0.1392	0.3490		
		3.112	0.1091	0.1009	0.0625	0.0198	0.0252	0.0088		

obvious that the ANN models possess higher ability to predict the mole fraction of both vapor and liquid phases with lower error levels. The model developed *via* ANN exhibits very good ability in determination of the both vapour and liquid compositions in the validation set, as witnessed by relatively low *RMSE* (in the range of 0.054—0.119) and high correlation coefficients (R^2=0.997 or greater). On the other hand, the RKS correlation, although it provided a quite satisfactory correlation in prediction, was less accurate than the ANN model (R^2 in the range of 0.980—0.990 and relatively higher *RMSE* of 0.115—0.546).

Since, once trained, the ANN can estimate VLE in a single step and is very useful where real-time estimation is required, particularly in real-time control. In contrast, EoS estimates the VLE iteratively. However, the ANN models require a large quantity of data of good quality, especially for complex polar systems (*i.e*. R23-CS_2), for training, otherwise the reliability of the model deteriorates.

REFERENCES

1 Petersen, R., Fredenslund, A., Rasmussen, P., "Artificial neural networks as a predictive tool for vapor liquid equilibrium", *Comput. Chem. Eng*., **18**, s63—s67(1994).

2 Guimaraes, P.R.B., McGreavy, C., "Flow of information through an artificial neural network", *Comput. Chem. Eng*., **19**(S1), 741—746 (1991).

3 Sharma, R., Singhal, D., Ghosh, R., Dwivedi, A., "Potential applications of artificial neural networks to thermodynamics: Vapour-liquid equilibrium predictions", *Comput. Chem. Eng*., **23**, 385—390(1999).

4 Ganguly, S., "Prediction of VLE data using radial basis function network", *Comput. Chem. Eng*., **27**, 1445—1454(2003).

5 Urata, S., Takada, A., Murata, J., Hiaki, T., Sekiya, A., "Prediction of vapor-liquid equilibrium for binary systems containing HFEs by using artificial neural network", *Fluid Phase Equilib*., **199**, 63—78(2002).

6 Mohanty, S., "Estimation of vapour liquid equilibria for the system carbon dioxide-difluoromethane using artificial neural networks", *Int. J. Refrig*., **29**, 243—249(2006).

7 Mohanty, S., "Estimation of vapour liquid equilibria of binary systems, carbon dioxid-ethyl caproate, ethyl caprylate and ethyle caprate using artificial neural networks", *Fluid Phase Equilib*., **235**, 92—98(2005).

8 Rai, P., Majumdar, G.C., Das Gupta, S., De, S., "Prediction of the viscosity of clarified fruit juice using artificial neural network: A combined effect of concentration and temperature", *J. Food Eng*., **68**, 527—533(2005).

9 Bouchard, C., Grandjean, A., "A neural network correlation for variation of viscosity of sucrose aqueous solutions with temperature and concentration", *Lebensm-Wiss. U. -Technol*., **28**, 157—159(1995).

10 Laugier, S., Richon, D., "Use of artificial neural networks for calculating derived thermodynamic quantities from volumetric property data", *Fluid Phase Equilib*., **210**, 247—255(2003).

11 Potukuchi, W., Wexler, A.S., "Predicting vapor pressures using neural networks", *Atmos. Environ*., **31**, 741—753(1997).

12 Shyam, S.S., Oon-Doo, B., Michele, M., "Neural networks for predicting thermal conductivity of bakery

products", *J. Food Eng*., **52**, 299—304(2002).
13 Rumelhart, D.E., Hinton, G.E., Williams, R.J., "Learning representations by backpropagation errors", *Nature*, **323**, 533—536(1986).
14 Hagan, M.T., Menhaj, M., "Training feedforward networks with the Marquardt algorithm", *IEEE Trans. Neural Networks*, **5**(6), 989—993(1994).
15 Minai, A.A., Willams, R.D., "Acceleration of back-propagation through learning rate and momentum adaptation", In: the 1st International Joint Conference on Neural Networks, 676(1990).
16 Haralambous, C., "Conjugate gradient algorithm for efficient training of artificial neural networks", *IEEE Proc*., **139**(3), 301—310(1992).
17 Karimi, H., Ghaedi, M., "Simultaneous determination of thiocyanate and salycilate by a combined UV-spectrophotometric detection principal component artificial neural network", *Ann. Chim*., **96**, 657—667(2006),
18 Fausett, L., "Fundamentals of Neural Networks: Architectures, Algorithms and Applications", Printice-Hall, New Jersey (1994).
19 Roth, H., Peters-Gerth, P., Lucas, K., "Experimental vapor-liquid equilibria in the systems R22-R23, R22-CO_2, CS_2-R22, R23-CO_2, CS_2-R23 and their correlation by equations of state", *Fluid Phase Equilib*., **73**, 147—166(1992).
20 Arbib, A. M., The Handbook of Brian Theory and Neural Networks, The MIT Press, Massachusetts, 15—20(2002).
21 Christov, M., Dohrn, R., "High-pressure fluid phase equilibria. Experimental methods and systems investigated (1994 — 1999)", *Fluid Phase Equilib*., **202**, 153 — 218(2002).
22 Soave, G., "Equilibrium constants from a modified Redlich-Kwong equation of state", *Chem. Eng. Sci*., **27**, 1197—1203(1972).